PHYSICAL-CHEMICAL PROPERTIES OF BISMUTH AND BISMUTH OXIDES: SYNTHESIS, CHARACTERIZATION AND APPLICATIONS

PROPIEDADES FÍSICO-QUÍMICAS DEL BISMUTO Y OXIDOS DE BISMUTO: SÍNTESIS, CARACTERIZACIÓN Y APLICACIONES

CLAUDIA MILENA BEDOYA HINCAPIÉ
Ing. Física, Universidad Nacional de Colombia – Sede Bogotá, cmbedoyahi@unal.edu.co

MANUEL JONATHAN PINZÓN CÁRDENAS
Ing. Mecatrónico, Universidad Nacional de Colombia – Sede Bogotá, mjpinzonc@unal.edu.co

JOSE EDGAR ALFONSO ORJUELA
PhD. Física, Universidad Nacional de Colombia – Sede Bogotá, jealfonsoo@unal.edu.co

ELISABETH RESTREPO PARRA
PhD. Ingeniería, Universidad Nacional de Colombia - Sede Manizales, erestrepopa@unal.edu.co

JHON JAIRO OLAYA FLOREZ
PhD. Materiales, Universidad Nacional de Colombia - Sede Bogotá, jjolayaf@unal.edu.co

Received for review March 10 th, 2012, accepted June 29th, 2012, final version July, 9 th, 2012

ABSTRACT: The physical-chemical properties of bismuth and its oxides have been studied over the last two decades. As a result of this research, the growth of these materials with different crystallographic structures, showing micro and nanometric dimensions has been achieved by using several techniques (cathodic pulverization, laser pulsed deposition and hydrothermal method, among others). The dimensions reached have enabled thin films, nanotubes, nanospheres and nanowires to be obtained, allowing the developing of devices such as heavy metal detectors, optical filters and magnetic field sensors. Due to the progress in these materials in recent years, in this work a bibliographical review was carried out of some techniques employed for processing bismuth based materials with nanometric dimension and some technological applications.

KEYWORDS: Bismuth, nanostructures, bismuth oxide, Aurivillius phases.

RESUMEN: Las propiedades físico-químicas del bismuto y sus óxidos han sido objeto de estudio en las dos últimas décadas. Como resultado de estas investigaciones, estos materiales se han logrado crecer en diferentes estructuras cristalográficas y con dimensiones micro y nanométricas, utilizando diferentes técnicas (pulverización catódica, depósito por laser pulsado, método hidrotérmico, etc). Las dimensiones alcanzadas han permitido obtener películas delgadas, nanotubos, nanoesferas y nanohilos, con los cuales se han desarrollado dispositivos entre los que se destacan detectores de metales pesados, filtros ópticos y sensores de campo magnético. Debido al auge que han tomado estos materiales en los últimos años, en este documento se realizó una revisión bibliográfica de algunas técnicas empleadas para procesar materiales basados en bismuto en forma nanométrica, y algunas de sus aplicaciones tecnológicas.

PALABRAS CLAVE: Bismuto, nanoestructuras, óxido de bismuto, fases Aurivillius.

1. INTRODUCTION

Nanomaterials (thin films, nanoparticles, nano-multilayers) have become important in the current development of material science [1-3]. One of the most used elements for these applications is bismuth. Bismuth is a semimetal with interesting electronic properties such as high carrier mobility, low effective mass, low carrier density, long mean free path; moreover, it is highly anisotropic in its Fermi level, presenting a high magnetoresistance [4]. These properties are due to the spatial arrangement of its atoms [5]. Some reports indicate that a transition from semimetal to semiconductor occurs for thin film thickness of approximately 28 nm [6]. This transition has been observed also in bismuth nanowires oriented in a specific direction (trigonal) for thicknesses close to 55 nm [7].

Also, nanostructured bismuth materials have generated a great deal of interest because of the quantum behavior produced by their size [8], making it very useful for applications such as magnetic field sensors, optical devices, thermoelectric coolers and power generators [4,8]. Because of its low toxicity, bismuth films have recently been used as electrodes in the detection of organic nitro compounds [9] and heavy metals [10], replacing mercury electrodes. Bismuth has also been used in cosmetics and pharmaceuticals in disinfectants, bacteriostatic agents and astringents as well as in the nuclear industry where it is used as a refrigerant [11].

2. BISMUTH-BASED SYSTEMS

The physicochemical properties of bismuth nanostructures differ from those presented in higher dimensions due to different structures such as wires and wells that show quantized states [12] and surface defects [13]. For instance, Bi in bulk has no thermoelectric properties due to electron and hole contributions canceling each other. However, quantum confinement effects have been demonstrated in nanowires with diameters below 50 nm, presenting thermoelectric properties with high efficiency for diameters close to 10 nm [14]. Some research groups have synthesized bismuth thin films [15], nanowires [16], nanotubes [17], nanoplates [18] and nanospheres [19] using different techniques, which will be presented.

2.1. Nanostructures

Bismuth nanoparticles have been widely exploited in heterogeneous catalysis, magnetic recording media, microelectronics, thermoelectric devices and lubrication [20,21].

Also, these hold outstanding tribological properties in presence of large charges [18]. A range of physicochemical methods recently applied to obtain nanoforms of bismuth have been studied, such as: cluster beam, laser ablation, pulsed laser vaporization, flame spraying, electron beam techniques, electron beam lithography, pulse electroplating techniques, including supercritical fluids and solution dispersion methods. The latter is a novel and simple method which has been used to obtain nanoparticles by using a suitable solvent [21]. Moreover, these structures have been synthesized using microwave irradiation for quality, simplicity, speed, low cost and the possibility to be processed at low temperatures [22]. Although this method is simple enough to use a domestic microwave oven and is most often performed in solution, the lack of control and understanding of microwave reaction variables in the process is a drawback to its widespread application [23]. Fig. 1 shows the transmission electron microscopy (TEM) image of a nanotube synthesized by this method in a vacuum

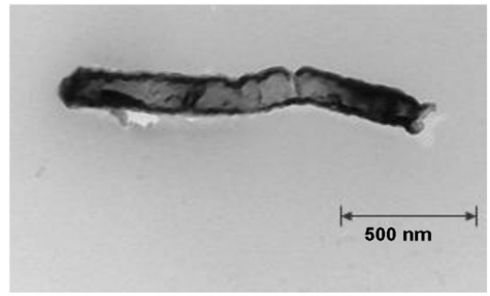

Figure 1. TEM Image of Bi nanotube [22]

Figures 2 and 3 present patterns of X-ray Diffraction (XRD) peaks of Bi nanoparticles and Bi_2O_3 nanorods. Bi nanoparticles obtained by thermal plasma change to nanorods when these are treated thermally at 250° C in atmosphere of oxygen by using different time intervals (2 and 3 hours) [24]. Figure 4 shows TEM micrographs of these nanostructures.

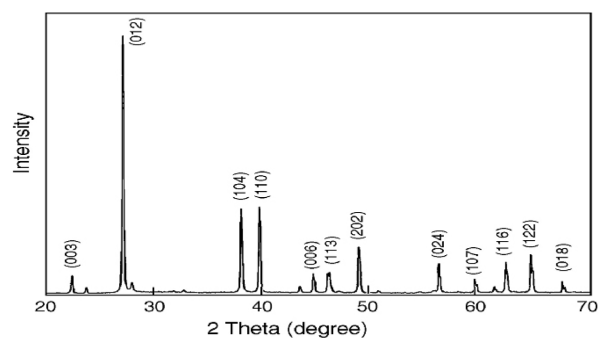

Figure 2. XRD diffractogram of Bi nanoparticles [24]

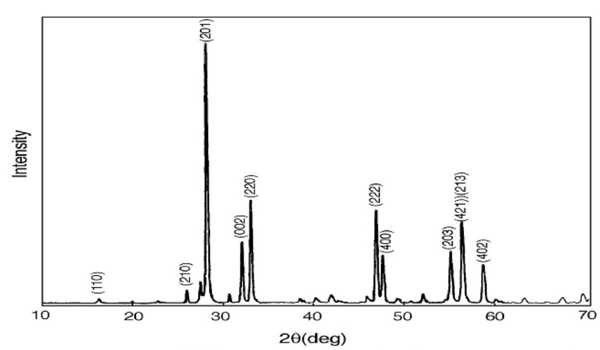

Figure 3. XRD diffractogram of Bi_2O_3 nanorods [24]

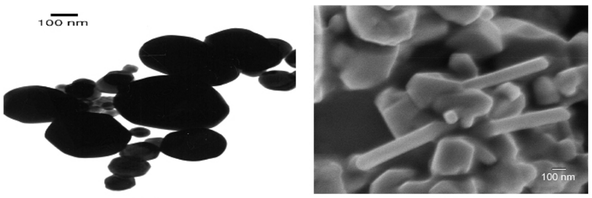

(a) **(b)**

Figure 4. (a) TEM image of Bi nanoparticles, (b) SEM image of Bi_2O_3 nanorods [24]

The formation of bismuth nanospheres was obtained on silicon wafers by a hydrothermal method [25]. Similarly, by means of an ethanol-thermal method bismuth nanobelts have been obtained from bismuth hydroxide on Si at 180°C for different reaction times (Fig. 5). The electrical properties of these nanobelts were measured from I-V curves, different properties from bulk bismuth materials were found. This study established that Bi nanobelts can be used as sensitive magnetic sensors or electronic nanodevices.

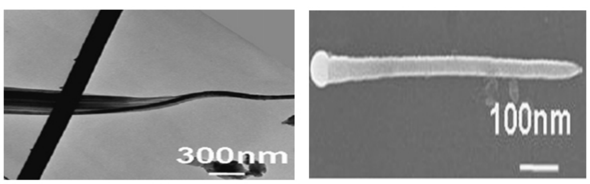

(a) **(b)**

Figure 5. Bi Nanobelts syntetized at 180 °C for different reaction times. (a) TEM image (5 h), (b) SEM Image (3h) [8]

On the other hand, the ultrafast optical response of glassy materials that contain metal nanoparticles has led to the fabrication of these materials doped with Au, Ag, Cu and Bi generally by melt quenching, sol-gel, sputtering, ion exchange, ion implantation and femtosecond laser irradiation Bismuth is very sensitive to preparation conditions. Growing this material on glass substrates is difficult; Geng Lin *et al.* in 2011 proposed a simple method to precipitate Bi nanoparticles on glass, using heat treatment processes and conventional melting [26].

2.2 Bismuth oxide (Bi_2O_3)

Bismuth oxide (Bi_2O_3), an important metal oxide semiconductor has been receiving considerable attention because it exhibits excellent optical and electrical properties such as wide band-gap, high refractive index, high dielectric permittivity and good photoconductivity [27]. Owing to these unique characteristics, bismuth oxides have been studied for use in various domains such as fuel cells, sensor technology, oxide varistors, ionic conductors [28,29], photoelectric materials, high temperature superconductors and functional ceramics [30]. Also it is an important component in the manufacturing of transparent ceramic glass, optical coatings [31], ceramics and catalysts [32]. Similarly, the industrial field of manufacturing technologies based on Bi_2O_3 optical fiber has advanced significantly as a result of a variety of high quality optical fiber production, such as bismuth oxide fiber doped with erbium (Er) and highly nonlinear bismuth oxide fibers[33].

Bi_2O_3 fibers are attractive because the material is about 200 times more nonlinear than SiO_2 [34]. These nonlinear phenomena play a key role in ultra-fast optical transmission systems and all -optical transport networks, therefore they can be investigated for use in all-optical processing sub-systems such as regenerators, demultiplexers, logic gates and optical switches. Semiconductors made from Bi_2O_3 have the benefit of compactness and integrability, even if they generally need temperature and current control and they are dynamically limited by charge carriers (hundreds of picoseconds). In the optical fibers, on the other hand, the nonlinear phenomena originated by Kerr effect are characterized by ultra-fast dynamics (few femtoseconds). The aim in recent studies has been to reduce the required fiber length with benefits in terms of compactness and polarization stability [35].

In recent years, several successful strategies including precipitation method, microwave-assisted synthesis, electrodeposition, and chemical vapor deposition (CVD), have been reported to prepare Bi_2O_3 with various morphologies, such as quantum dots, nanoparticles, nanobelts, nanorods, nanotubes nanofibers and thin films [28].

2.2.1. Bi_2O_3 phases

Bi_2O_3 is a complex system with four main polymorphs: α (monoclinic), β (tetragonal), γ (body-centered cubic) and δ (face-centered cubic), each one with unique physical properties [28] (electrical, optical, photoelectrical, etc.). For example at 300 K, the band gap E_g of α-Bi_2O_3 is equal to 2.85 eV, while for β phase is 2.58 eV [36]. Properties of bismuth oxide, Bi_2O_3, have been studied in recent years, since its monoclinic structure is one of the most important materials for synthesizing a number of high-temperature superconductors and Bi-containing ferroelectric compounds [37]. Particularly, the high applicability of δ phase is well known because of its high oxygen ionic conductivity [38]. This property is due to the quarter of the oxygen sites that are vacant in the fluorite-type lattice, according to Mairesse [39]; the electronic structure of Bi^{3+} is characterized by the presence of $6s^2$ pair electrons, leading to high polarisability of the cation lattice, oxide ion mobility and the ability of the Bi^{3+} to accommodate highly disordered surroundings.

2.2.2. Bi_2O_3 nanowires

Nanostructured materials, especially, semiconductor nanowires have attracted great attention recently becoming one of the most active research projects in the nanoscience area [40]. One of the most interesting structures is the nanowire of Bi_2O_3, because of its physical properties, such as, high refractive index ($n_{\delta Bi2O3}$=2.9) [41], dielectric permittivity (ε_r=190) and oxygen ionic conductivity (1.0 S/cm), as well as a remarkable photoconductivity and photoluminescence response [42]. Although some reports about synthesis and applications of Bi_2O_3 nanowires can be found, transition phases within polymorphisms is not studied enough. These studies are important for improving their applications in optical elements and storage devices, among others [43].

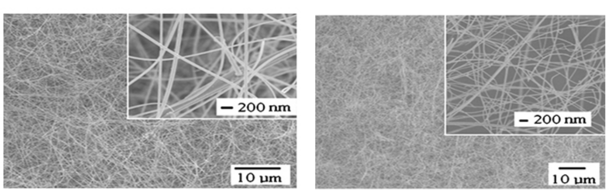

(a) (b)

Figure 6. SEM images of nanowires (a) α-Bi_2O_3, (b) β-Bi_2O_3 [42]

The phase transitions of α- and β- to δ and δ – to liquid phases for Bi_2O_3 nanowires were obtained recently by using the oxidative metal vapor transport deposition technique which exploits spatial-temporal separation of Bi evaporation, vapor transport, droplet formation, and oxidative nucleation and growth [44]. Results showed the size effect only for the δ to liquid phase, decreasing its transition temperature. In Fig. 6 SEM images of α- and β synthesized polymorphisms are presented, showing that the α- Bi_2O_3 phase (Fig. 6 (a)) consists of uniform nanowires close to 100 nm in diameter and several hundreds of micrometers in length. On the other hand, as is shown in Fig. 5(b), β-Bi_2O_3 contains exclusively ultrathin nanowires about 10 nm in diameter and several μm in length [43].

Until now, bismuth oxide nanowires have been successfully synthesized by different techniques including metalorganic chemical vapor deposition-MOCVD, chemical methods, and oxidative metal vapor transport deposition. These techniques employ high temperatures and chemical reaction routes in solid state, which are energetically intensive and their integration into silicon-based microelectronic devices is difficult. Therefore, bismuth nanowires with a high crystalline quality have been prepared using a novel method of induced stress at low temperatures on silicon substrates and subsequently annealed at low temperature in an oxygen environment [28].

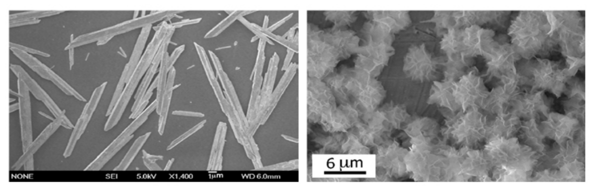

(a) (b)

Figure 7. SEM images (a) oblique prism-like α-Bi_2O_3, (b) Bi_2O_3 nanoflowers [28]

Also, oblique prim-like α-Bi_2O_3 phase was prepared by a simple one-step aqueous method at low temperature (50 °C) and ambient pressure. This method is suitable for industrial production because complex systems or conditions are not required [30]. Other geometries as Bi_2O_3 flower-shape has been successfully synthesized via a citric acid assisted hydrothermal process consisting of several nanosheets and nanoparticles [28]. These structures are illustrated in fig. 7.

2.2.3. Bismuth oxide Layers

Bismuth oxides have been considered as an interesting material because of their dielectric properties and have been used for applications such as optical coatings, metal-insulator-semiconductor capacitors and microwave-integrated circuits. There is also a general motivation to study bismuth oxides deposited as thin films, since bismuth is a common constituent of high-T_c superconductors such as $Bi_2Sr_2CaCu_2O_{8+x}$ and ferroelectrics such as $SrBi_2Ta_2O_9$ and $Bi_4Ti_3O_{12}$ [45]. In addition, Aurivillius phases are known for exhibiting ferroelectric behavior, most of the current ferroelectric materials show bismuth layered structures useful for non volatile random access memories. Other Aurivillius phases also present several properties and applications in photoluminescence devices [46] and oxygen ionic conduction [47]. Recently, it was found that these structures are efficient photo catalysts for separating water and degrading organic compounds. For instance, Kim et al. discovered that $PbBi_2Nb_2O_9$ is a suitable photocatalyst for separating water into O_2 and H_2. Moreover, it is useful for degrading isotropic alcohol to CO_2 [48] under visible light and recently they have been used in applications like humidity sensors using compounds like Bi_2MO_6 (M=W, Mo) because of high sensitivity, fast response and good reproducibility properties [49]. These Aurivillius structures are well described by superposition of $(B_2O_2)^{2+}$ layers and $(A_{n+1}B_nO_{3n+1})^{2-}$ blocks of perovskites [50], where A corresponds to mono- di- or trivalent elements with coordination number 12 (Na^+, Sr^{2+}, Ba^{2+}, Pb^{2+}, Ca^{2+}, Bi^{3+}); B is the transition cation suitable for an octahedron with lower size (Ti^{4+}, V^{5+}, Ta^{5+}, Nb^{5+}, W^{6+}, etc.) and *n* is an integer number representing the number of BO_6 octahedron in the perovskite layer along the packing direction. Fig. 8 presents representative structures for $BiWO_6$ (*n*=1), $SrBi_2Ta_2O_9$ (SBT, *n*=2) and $Bi_4Ti_3O_{12}$ (BIT, *n*=3). The perovskite layer is considered to be responsible for the ferroelectric behavior due to the presence of transition metal cations g[51]. These compounds are also known as BLSF (Bismuth layered-structure ferroelectrics) and they are characterized by having a high Curie temperature [49] and a strong anisotropy in their dielectric and ferroelectric properties as dielectric constant, remanent polarization and coercive field related to the crystalline structure [52]. Their spontaneous polarization (P_S) can be determined by *n*; if *n* is an even number, the material only exhibits *Ps* along the *a* axis by the symmetry and sliding planes perpendicular to the *b* and *c* axes. On the other hand, if *n* is odd, a lower *Ps* is produced along the *c* axis and a greater *Ps* occurs along *a* axis when the sliding planes are perpendicular [53]. The high transition temperature from a high symmetry phase (paraelectric state) to a low symmetry phase (ferroelectric state) encourages the use of these materials in the fabrication of capacitors, sensors, memory storage devices, optical displays and other electro-optical devices using condensers, transductors [54,55].

Several Aurivillius ceramic compounds have been synthesized and most of them have been examined for the substitution of Pb by Bi [56]. The study of these structures has been focused on the properties of *n* (*n*=2, 3, 4) oxides, with the compounds with $n \geq 5$ the least studied [52]. For applications in piezoelectricity and information storage, the effect of rare earth isovalent ions substitution as La^{3+}, Nd^{3+}, Sm^{3+}, Pr^{3+} in Bi^{3+} perovskite block sites improves the remanent polarization *Pr* and the fatigue resistance. The inclusion of ions like Na^+ or K^+ produces charge compensation effects: oxygen vacancy formations, valence state modification or interstitial site formations that influence the dielectric constant, polarisability and electric conductivity. These studies have been recently applied to the influence Na in the $Bi_4Ti_3O_{12}$ structure obtained by MOCVD, presenting a decrease in the lattice parameter in comparison with $Bi_4Ti_3O_{12}$ and a charge compensation caused by changes in Bi valence state, from Bi^{3+} to Bi^{5+} around Na [57].

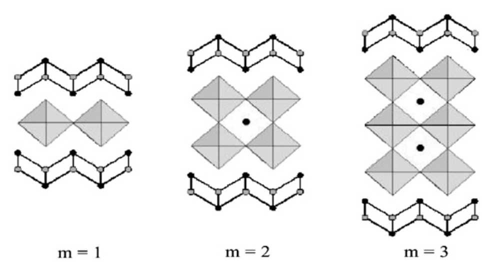

Figure 8. Schematic illustration of the Aurivillius phase structures [58]

Only a few BLSF compounds exhibit relaxation ferroelectric properties as $BaBi_2Nb_2O_9$ (BBN), $BaBi_2Ta_2O_9$ (BBT) and $K_{0.5}La_{0.5}Bi_2Ta_2O_9$. This behavior is characterized by a wide dielectric peak which shows a strong dependence on the frequency, possibly due to the microscopic distortion in the macroscopic tetragonal lattice and the disorder in the cations position [59]. The growth of these layered compounds has been carried out by several techniques such as metalorganic chemical vapor deposition (MOCVD), solid state synthesis and chemical etching methods [53, 56-66]. New phases of these materials have been successfully explored and produced [67-71]. A simple method for $Bi_{3.64}Mo_{0.36}O_{6.55}$ (BMO) nanoparticles fabrication with microwave irradiation and a hybridization with carbon through the combination of hydrothermal and calcination processes have been proposed by Fang Duan et al. in 2011 [72].

The flexibility in the cations accommodation or a combination of them is a special characteristic of Aurivillius oxides. In this way, in these research works one or more perovskite blocks have been inserted to obtain highly complex structures synthesizing by means of the solid state reaction route [73]. Such a method has several drawbacks, mainly poor homogeneity and hence required additional heat treatment and repeated grinding to obtain a nearly pure phase. Generally, the solid state reactions are diffusion controlled, and can be speeded up by prior usage of very fine particles and homogenized ingredients [74].

Future applications in photoluminescence have been investigated in BLSFs compounds such as $Bi_4Ti_3O_{12}$, Bi_3TiNbO_9, $SrBi_2Nb_2O_9$, $SrBi_2Ta_2O_9$, $CaBi_4Ti_4O_{15}$ and Bi_2WO_6, doped with rare earth (Eu, Er, Tm, etc). Deng Peng et al. in 2012 synthesized $CaBi_2Ta_2O_9$ doped with several concentrations of Pr by means of the solid state reaction method. The photoluminescence investigated with a blue light of 450 nm was improved with the substitution of Ca by Sr [75]. On the other hand, the introduction of magnetic transition metallic cations into the perovskite layer in the Aurivillius phases has been received with great interest since a new material named multiferroionics including ferroelectric and ferromagnetic effects [51], which involve local spin ordering and distorted structures with respect to the charge center [75]. Multiferroionic research has been mainly focused on modeling systems, such as perovskites with chemical formula ABO_3 (ferrites-bismuth, magnetite-bismuth) and in Aurivillius structures [49]. Multiferroionic materials as $BiFeO_3$, $Bi_5Ti_3FeO_{15}$, $Bi_6Ti_3Fe_2O_{18}$, $BiCrO_3$ and $BiMnO_3$ can be employed in a wide range of applications, as in the spintronics for multiple state memories elements [76], magnetically modulated piezoelectric transductors and resonance devices [77].

Experimentally, the production of these compounds by the conventional solid state reaction method has been widely used, taking into account important aspects as the possible formation of other phases because of the presence of ions with different valences. The conventional solid state reaction method also presents other disadvantages such as low reactant mixtures of homogeneity and a low ionic diffusion. Moreover, bismuth oxides are volatile and the reactivity between Ti^{4+}, or Nb^{5+} and Mn^{3+} in the solid state is different, producing compositional changes or defects in the Bi_2O_2 layers. Nevertheless, some Aurivillius phases containing Ti^{4+} or Nb^{5+} and Mn^{3+} produced by this method have been reported [78]. Compounds with highly distorted structures with meta-stable phases as $BiMnO_3$ have been synthesized by high pressure methods [79]. The n=4 Aurivillius phase, $Bi_5Ti_3CrO1_5$, prepared through solid state reaction by A.T. Giddings et al. (2011) show that the ferroelectricity and paramagnetism with short range antiferromagnetic coupling of the magnetic moments, inhibit it the long range magnetic ordering, therefore, this multiferroic material, is not suitable to be used in new technological applications [80].

In the last years, non conventional methods such as molten salt flux technique have been successfully reported for producing Aurivillius phases reaching high homogeneity in the precursor mixture. The molten salt can act as an environment for facilitating the reactive dissolution in order to obtain a homogenous mixture due to the incorporation of the salt medium So products generally possess a good crystallinity and crystalline morphology [51].

2.4. Other materials

Other phases known by their potential technological applications are compounds belonging to the $A_2B_2O_7$ family with pyrochlore structures. The $Bi_2Ti_2O_7$ phase with sphere shapes has been obtained by hydrothermal processes with variations in the hydroxide ions concentration [81]. On the other hand, the selenite phases with general formula $Bi_{12}MO_{20}$ (M=Ge, Ti, Ga, Fe, V, etc) exhibit several characteristics such as photo-refractivity, optical activity, photoconductivity and improved sound wave propagation velocity with applications in electro-optics, acoustic and piezoelectric devices [82]. Spherical nanoparticles of $Bi_{12}TiO_{20}$ have been obtained by means of hydrothermal treatment using $C_6H_{13}BiN_2O_7$ as a source of Bi, and $TiCl_3$ as a source of Ti for solving the agglomeration problems that normally occurs in the conventional hydrothermal method [83].

3. CONCLUSIONS

In this review work, properties and production techniques of nanostructure materials based on Bi and Bi oxides have been presented and described. This review is carried out in order to give to the readers a wide outlook of these materials, identifying their properties and potential technological applications.

REFERENCES

[1] Nieto, J., Caicedo, J., Amaya, C., Moreno, H., Aperador, W., Tirado, L. and Bejarano, G., Evaluación de la Influencia del voltaje Bias sobre la resistencia a la corrosión de películas delgadas de AlNbN, revista Dyna, 162, pp. 161-168, 2010.

[2] Olaya Flórez, J. J. and Marulanda, D., Propiedades eléctricas de nano-multicapas de Cr/CrN producidas por la Técnica de Sputtering con Magnétrón Desbalanceado, revista Dyna, 168, pp. 53-57, 2011.

[3] Tobón, J. I., Restrepo, O. J. and Payá Bernabeu, J.J., Adición de Nanopartículas al Cemento Portland, revista Dyna, 152, pp. 277-291, 2007.

[4] Du, X., Tsai, S., Maslov, D.L. and Hebard, A.F., Metal – Insulator - Like Behavior in Semimetallic Bismuth and Graphite, Phys. Rev. Lett., 94, pp. 166601-166604, 2005.

[5] Postel, M. and Duñach, E., Bismuth derivatives for the oxidation of organic compounds, Coordin. Chem. Rev., 155, pp. 127-144, 1996.

[6] Gribanov, E.N., Markov, O.I. and Khripunov, Y.V., When does Bismuth become a semimetal?, Nanotechnologies in Russia, 6, pp. 536-596, 2011.

[7] Konopko, L., Huber, T. And Nikolaeva, A., Quantum Interference and surface states effects in Bismuth nanowires, J. Low Temp. Phys., 158, pp. 523-529, 2010.

[8] Gao, Z., Qin, H., Yan, T., Liu, H. and Wang, J., Structure and resistivity of bismuth nanobelts in situ synthesized on silicon wafer through an ethanol-thermal method, J. Solid State Chemistry, 184, pp. 3257–3261, 2011.

[9] Timur, S. And Anik, Ü., α-Glucosidase based bismuth film electrode for inhibitor detection, Anal. Chim. Acta, 598, pp. 143-146, 2007.

[10] Lee, G.-J., Kim, C. K., Lee, M. K. and Rhee, C. K., Effect of phase stability degradation of bismuth on sensor characteristics of nano-bismuth fixed electrode. Talanta, 83, pp. 682-685, 2010.

[11] Chen, H.Y., Wu, L., Ren, C., Luo, Q.Z., Xie, Z.H., Jiang, X., Zhu, S.P., Xia, Y.K. and Luo, Y.R., The effect and mechanism of bismuth doped lead oxide on the performance of lead-acid batteries, J. Power Sour., 95, pp. 108-118, 2001.

[12] Hofmann, Ph., The surfaces of bismuth: Structural and electronic properties, Prog. Surf. Sci., 81, pp. 191-245, 2006.

[13] Albella, J.M., Láminas delgadas y recubrimientos: preparación, propiedades y aplicaciones, Solana e Hijos A.G., Madrid, 2003.

[14] Lin, Y.-M., Sun, X. and Dresselhaus, M.S., Theoretical investigation of thermoelectric transport properties of cylindrical Bi nanowires. Phys. Rev. B, 62, pp. 4610-4623, 2000.

[15] Song, D. W., Shen, W.-N., Dunn, B., Moore, C.D., Goorsky, M.S., Radetic, T., Gronsky, R. and Chen, G., Thermal Conductivity Of Nanoporous Bismuth Thin Films, Appl. Phys. Lett., 84, pp. 1883-1885, 2004.

[16] Hasegawa, Y., Ishikawa, Y., Komine, T., Huber, T.E., Suzuki, A., Morita, H. And Shirai, H., Magneto-Seebeck Coefficient Of A Bismuth Microwire Array In A Magnetic Field, Appl. Phys, Lett., 85, pp. 917-919, 2004.

[17] Yang, B., Li, C., Hu, H., Yang, X., Li, Q. and Qian, Y., A room- temperature route to bismuth nanotube arrays, Eur. J. Inorg. Chem., 2003, pp. 3699-3702, 2003.

[18] Fu, R., Xu, S., Lu, Y-N. and Zhu, J-J., Synthesis and Characterization of Triangular Bismuth Nanoplates, J. Cryst. Growth Des., 5(4), 1379-1385, 2005.

[19] Wang, J., Wnag, X., Peng, Q. and Li. Y. Synthesis and Characterization of Bismuth Single-Crystalline Nanowires and Nanospheres, Inorg. Chem., 43(23), pp. 7552-7556, 2004.

[20]Rohr, O., Bismuth - the new ecologically green metal for modern lubricating engineering, Ind. Lubr. Tribol., 54, pp. 153-164, 2002.

[21] Zhao, Y., Zhang, Z. and Dang, H., A simple way to prepare bismuth nanoparticles, Mater. Lett., 58, pp. 790-793, 2004.

[22] Kharissova, O. V., Osorio, M., Kharisov, B. I., Yacamán, M.J. and Ortiz Méndez, U., A comparison of bismuth

nanoforms obtained in vacuum and air by microwave heating of bismuth powder, Mater. Chem. Phys., 121, pp. 489-496, 2010.

[23] Mastrovito, C., Lekse, J.W. and Aitken, J. A., Rapid solid-state synthesis of binary group 15 chalcogenides using microwave irradiation. J. Solid State Chem., 180, pp. 3262-3270, 2007.

[24] Wang, L., Cui, Z.-L. and Zhang, Z.-K., Bi nanoparticles and Bi_2O_3 nanorods formed by thermal plasma and heat treatment, Surf. Coat. Tech., 201, pp. 5330-5332, 2007.

[25] Liu, H. and Wang, Z.L., Bismuth spheres grown in self-nested cavities in a silicon wafer, J. Am. Chem, Soc., 127, pp. 15322-15326, 2005.

[26] Lin, G., Tan, F., Luo, F., Chen, D., Zhao, Q. and Qiu, J., Linear and nonlinear optical properties of glasses doped with Bi nanoparticles.

J. Non-Crystalline Solids, 357, pp. 2312-2315, 2011.

[27]Leontie, L., Caraman, M., Delibas, M. and Rusu, G.I. Optical properties of bismuth trioxide thin films. Mater. Res. Bull., 36, pp. 1629-1637, 2001.

[28] Zhang, L., Hashimoto, Y., Taishi, T., Nakamura, I. and Ni, Q.-Q., Fabrication of flower-shaped Bi_2O_3 superstructure by a facile template-free process, Appl. Surf. Sci., 257, pp. 6577-6582, 2011.

[29] Nowak-Wozny, D., Janiczek, T., Mielcarek, W. and Gajewski. J.B., Fractional electrical model for modified bismuth oxide. J. Electrostatics, 67, pp. 18-21, 2009.

[30]Wang, Y., Zhao, J. and Wang. Z., A simple low-temperature fabrication of oblique prism-like bismuth oxide via a one-step aqueous process, Colloid Surface A, 377, pp. 409-413, 2011.

[31] Schuisky, M. and Härsta, A., Epitaxial growth of $Bi_2O_{2.33}$ by halide Cvd, Chem. Vap. Depos., 2(6), pp. 235-238, 1996.

[32]Li, L., Yang, Y., Fang, X., Kong, M., Li, G., Zhang., L., Diameter-dependent electrical transport properties of bismuth nanowire arrays. Communications, 141, pp. 492-496, 2007.

[33] Lee, J.H., Ohara, S., Nagashima, T., Hasegawa, T., Sugimoto, N., Igarashi, K., Katoh, K. and Kikuchi, K., Clock Recovery and Demultiplexing of High-Speed OTDM Signal Through Combined Use of Bismuth Oxide Nonlinear Fiber and Erbium-Doped Bismuth Oxide Fiber, IEEE Photonic Tech L., 17, pp. 2658-2660, 2005.

[34] Vedadi, A., Jamshidifar, M. and Marhic, M. E., Continuous-Wave Bismuth-Oxide One-Pump Fiber Optical Parametric Amplifier, 34th European Conference On Optical Communication (ECOC 2008), IEEE, Brussels, 2008.

[35] Scaffardi, M., Fresi, F., Meloni, G., Bogoni, A., Poti, L. and Calabretta, N., 160 Gbit/s OTDM demultiplexer exploiting 1-meter-long bismuth oxidebased fiber, in Proc. IEEE LEOS Annu. Meeting, pp. 918-919, 2005.

[36] Leontie, L., Caraman, M., Alexe, M. and Harnagea, C., Structural and optical characteristics of bismuth oxide thin films. Surf. Sci., 507-510, pp. 480-85, 2002.

[37] Orlov, V. G., Bush, A. A., Ivanov, S. A. and Zhurov, V.V., Anomalies in the physical properties of the α form of bismuth oxide. Phys. Solid State, 39(5), pp. 770-774,1997.

[38] Sammes, N. M., Tompsett, G. A., Naè Fe, H. and Aldingera, F., Bismuth Based Oxide Electrolytes- Structure and Ionic Conductivity. J. Eur. Ceramic Society, 19, pp. 1801-1826, 1999.

[39]Mairesse, G., In Fast Ion Transport in Solids, ed. B. Scrosati, Kluver, Amsterdam, 271, 1993.

[40] Mei, Z.W., Liu, Y., Wang, H., Gao, S.J., Wen, X.G., Gu, L., Qiu, Y.F. and Yang, S.H., Facile and Controllable Growth of ZnO 1D Nanostructure Arrays on Zn Substrate by Hydrothermal Process, J. Nanosci. Nanotechnol., 10, 3123-30, 2010.

[41]Fan, H.T., Teng, X.M., Pan, S.S., Ye, C., Li, G.H. and Zhang, L.D., Optical properties of δ-Bi_2O_3 thin films grown by reactive sputtering, Appl. Phys. Lett., 87, pp. 231916-231918, 2005.

[42] Greenberg, Y., Yahel, E., Caspi, E.N., Benmore, C., Benuneu, B., Dariel, M.P. and Makov, G. Evidence for a temperature-driven structural transformation in liquid bismuth, Europhysics Lett., 86, 36004, 2009.

[43] Qiu, Y., Yang, M., Fan, H., Zuo, Y., Shao, Y., Xu, Y., Yang, X. and Yang, S., Phase-transitions of α- and β-Bi_2O_3 nanowires. Mater. Lett., 65, pp. 780-782, 2011.

[44] Qiu, Y., Liu, D., Yang, J. and Yang, S., Controlled Synthesis of Bismuth Oxide Nanowires by an Oxidative Metal Vapor Transport Deposition Technique, Adv. Mater., 18, pp. 2604-2608, 2006.

[45] Kang, S.W. and Rhee, S.W., Growth of bismuth oxide films by direct liquid injection-metal organic chemical vapor deposition with Bi(tmhd)3 (tmhd: 2,2,6,6-tetramethyl-3,5-heptanedione). Thin Solid Films, 468, pp. 79-83, 2004.

[46] Ida, S., Ogata, C., Unal, U., Izawa, K., Inoue, T., Altuntasoglu, O. and Matsumoto, Y., Preparation of a Blue Luminescent Nanosheet Derived from Layered Perovskite $Bi_2SrTa_2O_9$, J. Am. Chem. Soc., 129, pp. 8956-8957, 2007.

[47] Yasuda, N., Miyayama, M. and Kudo, T., Oxide ion conductivity of bismuth layer-structured $Bi_2K_{1-x}Nb_2O_{8.5-\delta}$, Solid State Ionics, 133, pp. 273-278, 2000.

[48] Kim, H.G., Hwang, D.W. and Lee, J.S., An undope, single-phase oxide photocatalyst working under visible light, J. Am. Chem. Soc., 126, pp. 8912-8913, 2004.

[49] Zheng, K., Zhou, Y., Gu, L., Mo, X., Patzke, G. R. and Chen, G., Humidity sensors based on Aurivillius type Bi_2MO_6 (M=W, Mo) oxide films. Sensors and Actuators B, 148, pp. 240-246, 2010.

[50] Suhua, F., Wen, C., Fengqing, Z. and Guangda, H., Effects of Excess Bismuth on Structure and Properties of $SrBi_4Ti_4O_{15}$ Ceramics. Journal of Rare Earths, 25, pp. 317-321, 2007.

[51] Zulhadjri, Prijamboedi, B., Nugroho, A.A., Mufti, N., Fajar, A., Palstra, T.T.M. and Ismunandar. Aurivillius phases of $PbBi_4Ti_4O_{15}$ doped with Mn^{3+} synthesized by molten Salt technique: Structure, dielectric, and magnetic properties. J. Solid State Chemistry, 184, pp. 1318-1323, 2011.

[52] Jin, S., Miranda Salvado, I. M. and Costa, M. E., Structure, dielectric and ferroelectric anisotropy of $Sr_{2-x}Ca_xBi_4Ti_5O_{18}$ ceramics. Mater. Res. Bull., 46, pp. 432-437, 2011.

[53]Watanabe, T. and Funakubo, H., Controlled crystal growth of layered-perovskite thin films as an approach to study their basic properties. J. Appl. Phys., 100, 051602-11, 2006.

[54]Anlin Golda, R., Marikani, A. and Pathinettam Padiyan, D., Mechanical synthesis and characterization of $Bi_4Ti_3O_{12}$ nanopowders. Ceram. Int., 37, pp. 3731-3735, 2011.

[55] Jardiel, T., Caballero, A.C. and Villegas, M., Aurivillius ceramics: $Bi_4Ti_3O_{12}$-based piezoelectrics. J. Ceramic Society of Japan, 116(4), pp. 511-518, 2008.

[56]Henriques, E.I., Kim, H.J., Haluska, M.S., Edwards, D.D. and Misture, S.T., Solid solubility and electrical conduction mechanisms in 3-layer Aurivillius ceramics, Solid State Ionics, 178, pp. 1175-1179, 2007.

[57] Schwarzkopf, J., Dirsyte, R., Devi, A., Kwasniewski, A., Schmidbauer, M., Wagner, G., Michling, M., Schmeisser, D. and Fornari, R., Influence of Na on the structure of $Bi_4Ti_3O_{12}$ films by liquid-delivery spin MOCVD, Thin Solid Films, 519, pp. 5754-5759, 2011.

[58] Pirovano, C., Saiful Islam, M., Vannier, R.-N., Nowogrocki, G. and Mairesse, G., Modelling the crystal structures of Aurivillius phases. Solid State Ionics, 140, pp. 115-123, 2001.

[59] Du, H., Li, Y., Shi, X. and Liu, C., Relaxor behavior of bismuth layer-structured ferroelectric ceramic with m=2, Solid State Commun., 148, pp. 357-360, 2008.

[60]Shen, Y., Clarke, D.R. and Fuierer, P.A., Anisotropic thermal conductivity of the Aurivillus phase, bismuth titanate $Bi_4Ti_3O_{12}$: A natural nanostructured superlattice. Appl. Phys. Lett., 93, 102907-3, 2008.

[61] Li, J.-B., Huang, Y. P., Rao, G. H., Liu, G. Y., Luo, J., Chen, J. R. and Liang, J. K., Ferroelectric transition of Aurivillius compounds $Bi_5Ti_3FeO_{15}$ and $Bi_6Ti_3Fe_2O_{18}$. Appl. Phys. Lett., 96, 222903 - 3, 2010.

[62] Jovalekic, C., Zdujic, M. and Atanasoska, LJ., Surface analysis of bismuth titanate by Auger and X-ray photoelectron spectroscopy. J. Alloys and Compounds, 469, pp. 441–444, 2009.

[63] Jardiel, T., Caballero, A. C., Fernández, J. F. and Villegas, M., Domain structure of $Bi_4Ti_3O_{12}$ ceramics revealed by chemical etching. J. European Ceramic Society, 26, pp. 2823-2826, 2006.

[64] Guo, D., Li, M., Wang, J., Liu, J., Yu, B. and Yang, B., Ferroelectric properties of $Bi_{3.6}Ho_{0.4}Ti_3O_{12}$ thin films prepared by sol-gel method, Appl. Phys. Lett., 91, 232905-3, 2007.

[65] Boffoue, M. O., Jacquot, A., Duclere, J.-R., Guilloux-Viry, M., Hejtmanek, J., Dauscher, A., and Lenoir, B., Thermal conductivity of $SrBi_2Nb_2O_9$ ferroelectric thin films, Appl. Phys. Lett., 89, 092904-3, 2006.

[66] Chia, W.-K., Chen, Y.-C., Yang, C.-F., Young, S.-L., Chiang, W.-T. and Tsai, Y.-T., Characteristics of $Bi_4Ti_3O_{12}$ thin films on ITO/glass and Pt/Si substrates prepared by R.F. sputtering and rapid thermal annealing, J Electroceram, 17, pp. 173-177, 2006.

[67]Wang, D., Tang, K., Liang, Z. and Zheng, H., Synthesis, crystal structure, and photocatalytic activity of the new three-layer aurivillius phases, $Bi_2ASrTi_2TaO_{12}$ (A=Bi, La), J. Solid State Chemistry, 183, pp. 361-366, 2010.

[68] Yu, J. and Kudo, A., Effects of Structural Variation on the Photocatalytic Performance of Hydrothermally Synthesized $BiVO_4$, Adv. Funct. Mater., 16, pp. 2163-2169, 2006.

[69]Fu, H., Zhang, S., Xu, T. and Zhu, Y., Photocatalytic Degradation of RhB by Fluorinated Bi_2WO_6 and Distributions of the Intermediate Products, J. Chen. Environ. Sci. Technol., 42, pp. 2085-2091, 2008.

[70]Masiukaite, E., Banys, J., Sobiestianskas, R., Ramoska. T., Khomchenko, V.A. and Kiselev, D.A., Conductivity investigations of Aurivillius-type $Bi_{2.5}Gd_{1.5}Ti_3O_{12}$ ceramics, Solid State Ionics, 188, pp. 50-52, 2011.

[71]Maczka, M., Ptak, M., Kepinski, L., Tomaszewski, P.E. and Hanuza, J., X-ray, SEM, Raman and IR studies of $Bi_2W_2O_9$ Prepared by Pechini method, Vib. Spectrosc., 53, pp.199-203, 2010.

[72] Duan, F., Zheng, Y. and Chen, M., Enhanced photocatalytic activity of bismuth molybdate via hybridization with carbon, Mater. Lett., 65, pp. 191-193, 2011.

[73] Kumar, S. and Varma, K.B.R., Structural, dielectric and ferroelectric properties of four-layer Aurivillius phase $Na_{0.5}La_{0.5}Bi_4Ti_4O_{15}$, Mater. Sci. Eng. B, 172, pp. 177-182, 2010.

[74] Halim, S.A., Khawaldeh, S.A., Mohamed, S.B. and Azhan, H. Superconducting properties of $Bi_{2-x}Pb_xSr_2Ca_2Cu_3O_y$ system derived via sol-gel and solid state routes, Mater. Chem. Phys., 61, pp. 251-259, 1999.

[75]Peng, D., Sum, H., Wang, X., Zhang, J., Tang, M. and Yao, T., Blue excite photoluminescence of Pr doped $CaBi_2Ta_2O_9$ based ferroelectrics, J. Alloys and Compounds, 511, pp. 159-162, 2012.

[76]Simoes, A.Z., Cavalcante, L.S., Riccardi, C.S., Varela, J.A. and Longo, E., Improvement of fatigue resistance on La modified $BiFeO_3$ thin films. Current Applies Physics, 9, pp. 520-523, 2009.

[77] Missyul, A.B., Zvereva, I.A., Palstra, T.T.M. and Kurbakov, A.I., Double-layered Aurivillius-type ferroelectrics with magnetic moments. Mater. Res. Bull., 45, pp. 546-550, 2010.

[78]Suresh, M.B., Ramana, E.V., Babu, S.N. and Suryanarayana, S.V., Comparison of electrical and dielectric properties of BLSF materials in Bi–Fe–Ti-O and Bi-Mn-Ti-O systems, Ferroelectrics, 332, pp. 57-63, 2006.

[79] Chi, Z.H., Xiao, C.J., Feng, S.M., Li, F.Y. and Jin, C.Q., Manifestation of ferroelectro-magnetism in multiferroic $BiMnO_3$, J.Appl.Phys., 98, 103519-5, 2005.

[80] Gidding, A.T., Stennett, M.C., Reid, D.P., Mccabe, E.E., Greaves, C. and Hyatt, N.C., Synthesis, structure and characterization of the n=4 Aurivillius phase $Bi_5Ti_3CrO_{15}$, J. Solid State Chemistry, 184, pp. 252-263, 2011.

[81] Hou, J., Jiao, S., Zhu, H. and Kumar, R.V., Bismuth titanate pyrochlore microspheres: Directed synthesis and their visible light photocatalytic activity, J. Solid State Chemistry, 184, pp. 154-158, 2011.

[82]Nippolainen, E., Kamshilin, A.A., Prokofiev, V.V. and Jaaskelainen, T., Combined formation of a self-pumped phase-conjugate mirror and spatial subharmonics in photorefractive sillenites, Appl. Phys. Lett., 78, 859-3, 2001.

[83] Zhu, X., Zhang, J. and Chen, F., Study on visible light photocatalytic activity and mechanism of spherical $Bi_{12}TiO_{20}$ nanoparticles prepared by low-power hydrothermal method, Appl. Catal. B: Environ., 102, pp. 316-322, 2011.